A Comparative Assessment of Dynamic and Conventional Thallium-201 SPECT Myocardial Perfusion Imaging: Monte Carlo Simulations and Case Studies

Zohreh Shahpouri[1], Alireza Kamali-Asl[1,*], Ahmad Bitarafan-Rajabi[2], Jakir Hossain[3], Seyed Mohammad Entezarmahdi[1], Samane Mohseni[1], Nahid Yaghoobi[4], Arman Rahmim[3,5]

1. Radiation Medicine Engineering Dept. Shahid Beheshti University, GC, Iran.
2. Cardiovascular Interventional Research Center; Department of Nuclear Medicine, Rajaei Cardiovascular, Medical & Research Center, Iran University of medical sciences, Iran.
3. Departments of Radiology & Radiological Science, Johns Hopkins University, School of Medicine, Baltimore, USA.
4. Department of Nuclear Medicine, Rajaei Cardiovascular, Medical & Research Center, Iran University of Medical Sciences, Iran.
5. Departments of Electrical & Computer Engineering, Johns Hopkins University, School of Medicine, Baltimore, USA.

Article info:
Received: January 17 2013
Accepted: March 06 2013

Keywords:
Dynamic SPECT,
Cardiac Perfusion Imaging,
Thallium.

ABSTRACT

Purpose: Clinical myocardial perfusion SPECT is commonly performed using static imaging. Dynamic SPECT enables extraction of quantitative as well as relative perfusion information. We aimed to evaluate the ability of dynamic SPECT for regular perfusion assessment in comparison to conventional SPECT in the context of thallium-201.

Methods: Simulations were performed utilizing a 4D-NCAT phantom for a dual-head gamma camera via the SIMIND Monte-Carlo simulator. 64s acquisition time-frames were used to track these dynamic changes. Different summations of time-frames were performed to create each dataset, which were compared to a standard static dataset. In addition, the effect of different delay-times post-injection was assessed. Twenty-segment analysis of perfusion was performed via the QPS analyser. Dynamic data were subsequently acquired in clinical studies using simulation-optimized protocols.

Results: For different summations of time-frames, perfusion scores in the basal and mid regions revealed 14.4% and 7.3% increases in dynamic SPECT compared to conventional imaging, with maximum changes in the basal anterior, while the distal and apical segments did not show noticeable changes. Specifically, dynamic imaging including 4 to 6 time-frames yielded enhanced correlation (R=0.957) with conventional imaging, in comparision to the usage of less time frames. Greatest correlation with conventional imaging was obtained for post-injection delays of 320 to 448s (R=0.982 to R=0.988).

Conclusion: While dynamic SPECT opens up an important opportunity for quantitative assessment (e.g. via generation of kinetic parameters), it was shown to generate highly consistent perfusion information compared to established conventional imaging. Future work focuses on merging these two important capabilities.

1. Introduction

The ability to extract functional information from organs in vivo has extensive implications both in the clinic and research. Single photon emission computed tomography (SPECT) and positron emission tomography (PET) imaging are recognized as powerful imaging techniques suited for investigation of organ function in three dimensions [1]. In the case of SPECT imaging, static scanning is routinely

** Corresponding Author:*
Alireza Kamali-Asl, PhD
Associate Prof. Radiation Medicine Engineering Department, Shahid Beheshti University, Tehran, Iran.
E-mail: a_r_kamali@yahoo.com / a_kamali@sbu.ac.ir

utilized to evaluate the activity distribution in the organs of interest. Physiological processes, however, are manifested with changing distributions of biological uptake over time.

In a static cardiac SPECT scan, the projection data is acquired in 180 degree over a period of 15 to 30 minutes. In order to acquire the parameters of time dependence, it was necessary to achieve projections in a shorter time [2, 3].The rate of such a change would provide important information for assessment of disease [4-8].

At present, myocardial perfusion SPECT imaging (MPI) is an appropriate method for diagnosis and prognosis of coronary artery disease (CAD) [9, 10]. Dynamic cardiac SPECT imaging method is one of the proposed methods in nuclear cardiology which has the potential to extract both kinetic and perfusion information for evaluation of CAD, and may provide more accurate measurement of myocardial stiffness development in comparison to static images [11-13].

The selected tracer to study tissue kinetics should entail active transport in the region of interest [14]. It has been demonstrated that teboroxime extraction reflects the true blood flow more accurately than other myocardial perfusion agents such as Tl-201 or Tc-99m MIBI [15-19]. However, teboroxime has very rapid kinetics, which requires very fast temporal sampling that is not feasible on most SPECT systems [20, 21]. The other most suitable choice is thallium-201 which is a potassium analog tracer and works in conjunction with the Na-K ATPase pump (Tl, half-life ≅ 73.5 h) [18, 22]. It undergoes high transcapillary extraction during the early uptake phase immediately following administration. It belongs to the III-A group and has similar but not identical potassium bio-kinetic properties. There is evidence that wash-in rate parameters estimated from dynamic thallium SPECT may provide accurate quantitative measures of myocardial blood flow. Few experimental studies have been performed on thallium kinetic parameter estimation [17, 19, 23].

Dynamic cardiac acquisition can be utilized to extract perfusion information similar to well-established conventional imaging. It can also provide kinetic information. Using summation of all tomographic data, perfusion imageswere created by Kadrmas for teboroxime and by Khare for thallium [24, 25]. Recently Gated dynamic cardiac SPECT imaging has been introduced which can extract the kinetic parameters. Besides, it has the capability of extracting the functional information [26-29]. So far, several studies have been performed in order to extract the kinetic parameter from the gated dynamic cadiac SPECT [30-38]. Therefore, it suggests that the dynamic SPECT imaging will be used in the clinics in the near future. In addition to the functioanl parameters and parametric maps, there is a need for an acceptable perfusion image.

A question we set to investigate is how the resulting perfusion image compares to conventional imaging. The focus of our research has thus been to perform careful comparisons between dynamic and conventional SPECT methodologies in myocardial perfusion assessment, demonstrating the ability of dynamic imaging to maintain conventional capabilities, and to move beyond. As such, different summations of dynamic cardiac SPECT data were performed to investigate the effect of start-time and total acquisition time as utilized in the dynamic imaging protocol.

2. Methods

2.1. Simulation Studies

To track the time-varying activity of the radioactive-labelled tracer injected into the body,dynamic projection sets were generated over a finite period of time as sufficient to assess temporal changes of the tracer [3].

We first generated time-varying activities for the ventricular blood pool and localized regions of the myocardial tissue. To do this, a two-compartment model [39] was used that generated the time–activity curves (TACs) in the plasma and myocardial regions based on rate constants for the exchange of tracer between the plasma and myocardial tissue.

This exchange between the blood concentration B(t) and the extravascular compartmental concentration C_EV (t)was modelled with the kinetic parameters K1 (wash-in) and k2 (wash-out), as shown in Fig. 1, given the following differential equation:

$$\frac{d}{dt}C_{EV}(t) = -k_2 C_{EV}(t) + K_1 B(t), \quad (1)$$

The solution is given by:

$$C_{EV}(t) = K_1 \int_0^t e^{-k_2 \tau} B(t-\tau)d\tau . \quad (2)$$

Equation (2) expresses that the tissue concentration is the convolution of the blood activity with an exponential kernel that is a function of the rate constants. For a known input function B(t), the model changes to a one compartmental model [4].

The tracer activity in the tissue depends on both the tissue activity and the fraction of blood f_v that is present in the myocardial region of interest. As such, the activity concentration in the region of interest at time point t, M(t), is given by:

$$M(t) = (1 - f_v)C_{EV}(t) + f_v B(t), \quad (3)$$

The right and left ventricular plasma activities were assumed nearly identical.

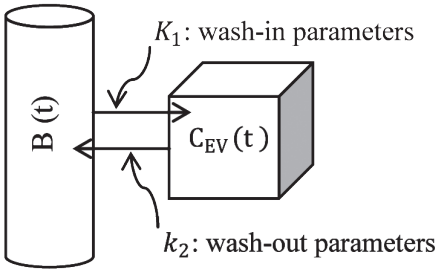

Figure 1. One-compartmental model used to represent the kinetics of 201-Tl distributions in the myocardium. As the blood activity is known, the blood is not treated as a separate compartment.

To create the time-varying organ activity in the region of interest, we used the Dynamic NURBS-based Cardiac-Torso (4D-NCAT) phantom with a tracer-kinetic model for thallium-201 labeled thallium chloride [40].

In myocardial perfusion SPECT in the present context of Tl, three physiological regions, namely the myocardium, blood pools and body (background) were simulated.

The wash-in and wash-out kineticparameters and conversion factor of plasma activity to blood utilized were based on experimental Tl studies,being 0.943 and 0.018, respectively [41, 42]. The Concentration of the other parts of the body was set to 10% of the myocardium activity at each time as a background activity. These TACs andan example slice through the simulated phantom are shown in Fig. 2.

Body dimensions were: 40.0 cm on long axis, 34.5 cm on transverse axis and 27.5 cm on AP axis.The phantom properties were: male, supine, 192 cm height and 95 kg weight.The image pixel size was 0.03125 cm, 128×128 matrix size, two sub-voxel and all simulation contain 128 slices [40].

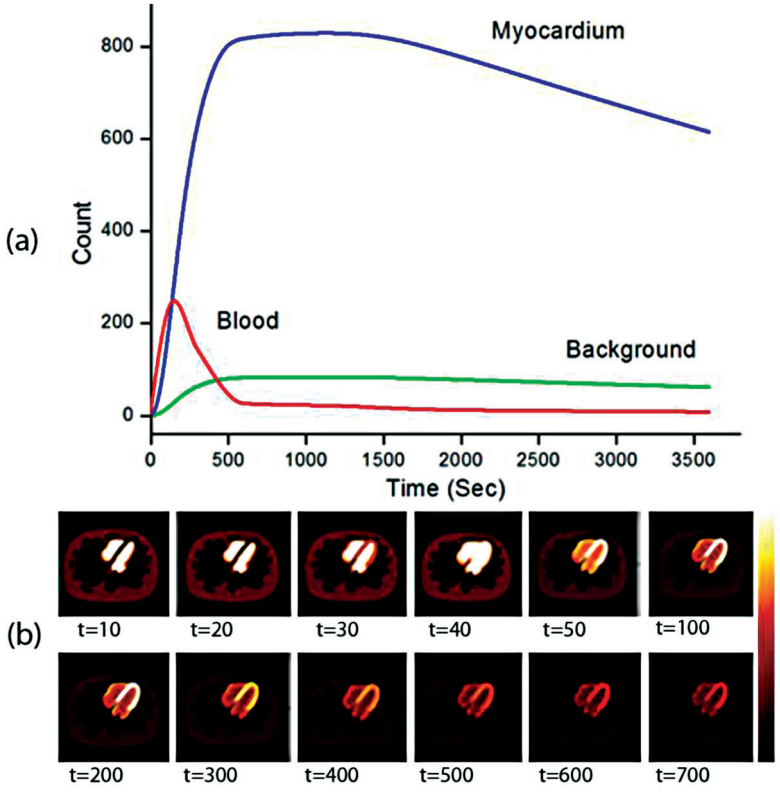

Figure 2. (a): An example of the TACs for blood pool, myocardium and background used in Tl 4D-NCAT simulations. **(b):** A typical transverse slice of the emission 4D-NCAT phantom at different times are shown in order from left to right.

We simulated a clinical 201-Tl study using the SIMIND (Simulating Medical Imaging Nuclear Detectors) simulator for the Siemens Simbia T series dual-head SPECT system. This validated Monte Carlo based software has been utilized to simulate SPECT systems and revised several time since 1996 [43-45].The field of view was 40.0 cm, resulting in a pixel size of 0.64 cm for a 64*64 pixels acquisition matrix.The continuous-step-and-shoot-mode was chosen [46].The LEHR collimator was selected (the hole diameters are 0.111 and 0.124 cm, with distances of 0.016 and 0.09 cm between the holes in X and Y dimensions, respectively). Sixty-four sec acquisition frames were used to track these dynamic changes. The Syngo software (version 2009), as installed on our SPECT system, was used to reconstruct and process the DICOM files.

To investigate and optimize the imaging protocol for evaluation of perfusion in dynamic SPECT, different summations of the variable time frames were performed to create each dataset, which were compared to a single static dataset (as commonly used in the clinic) with consistent projections as reference. In addition, the effect of different delay times after injection (time-step= 0 to 448 s in steps of 32 s) was assessed. Twenty-segment analysis of perfusion scores was performed using the QPS analyser (Cedars-Sinai Quantification Perfusion SPECT (QPS), 2009 version).

2.2. Case Studies

For improved assessment of the wash-in data, tracer injection was performed as a bolus injection on the SPECT table, as is commonly the case [47]. A bolus injection of 3.63±0.23 mCi 201-Tl was utilized, and scanning was performed on the above-mentioned dual-head SPECT system. The acquisition framework utilized in the simulated study was closely followed and implemented in the case studies. To do this, the camera gantry was continuously rotated at a high rotation speed yielding 180° coverage in 64s (32 views). Projection sets were acquired using three cycles, each of 64s, thus covering over 3 min, resulting in 96 dynamic projection sets.The acquisition delays post-injection for each case are shown in Table 3.

The rotation of the detectors was right anterior oblique. The imaging was performed along a non-circular path in continues mode, without cardiac gating. Two energy windows centered at 71 and 167 KeV (15% energy window width) were utilized for optimal performance [48]. The magnification factor and the imaging matrix size were set to 1.45 and 64*64, respectively. Case position was head-out and supine. The MLEM reconstruction method (4 iterations) was used for the reconstruction of clinical dynamic perfusion imaging. The clinical population studies included three cases . The first case, without any history of heart disease and both patients with prescribed viability test were referred to the nuclear medicine division of Shahid Rejaiee hospital for myocardial thallium scan.

It should be noted that the conventional imaging protocol was applied with no change in the amount of radiotracer injection(3.63±0.23 mCi 201-Tl). Before the start of imaging studies, the uniformity and other essential quality control tests were performed. The conventional imaging was performed in step-and-shoot-mode, with 32 projections, and other parameters were the same as the simulation studies (such as collimator, energy window, zoom factor, FOV, etc.). The conventional scans (rest Tl) began 15 to 20 minutes post-injection, for a duration of about 10 min. Case injections were performed under approved standards of medical ethics.

3. Results

3.1. Simulation Studies

Table 1 demonstrated the QPS quantification results of dynamic MPI in the context of Tl at 1 to 6 different time acquisition intervals (repeat of tomographic path). According to the QPS computation, for different summations of the time-frames, perfusion scores revealed maximal changes in mean perfusion values in the basal inferior and mid anterior regions. In these regions, dynamic SPECT revealed 19% and 12.8% increases, while the distal and apical segments showed slight decreases in comparison with the conventional method.

The correlation coefficient between dynamic and static images are shown in figure 3. Specifically, dynamic imaging with 4 to 6 time frames yielded enhanced correlation (R=0.957) with respect to values obtained using conventional imaging, in comparison to the usage of less time frames.

Generally, results between dynamic SPECT perfusion images and conventional SPECT images indicated high correlation between the two methods, especially when utilizing a high number of time-frames in dynamic imaging.

As shown in tables1 and 2, the correlation coefficient between simulated dynamic and static imaging using different start times was improved with increasing frames. The negative sign of the absolute difference percentage

of uptake values demonstarate a higer perfusion score in dynamic bull's eye map in comparison to the conventional one. The summing procedure that produced the best correlation with conventional image consisted of dynamic data acquired with a delay in the range 320 to 448 sec post-injection (R=0.982 to R=0.988).

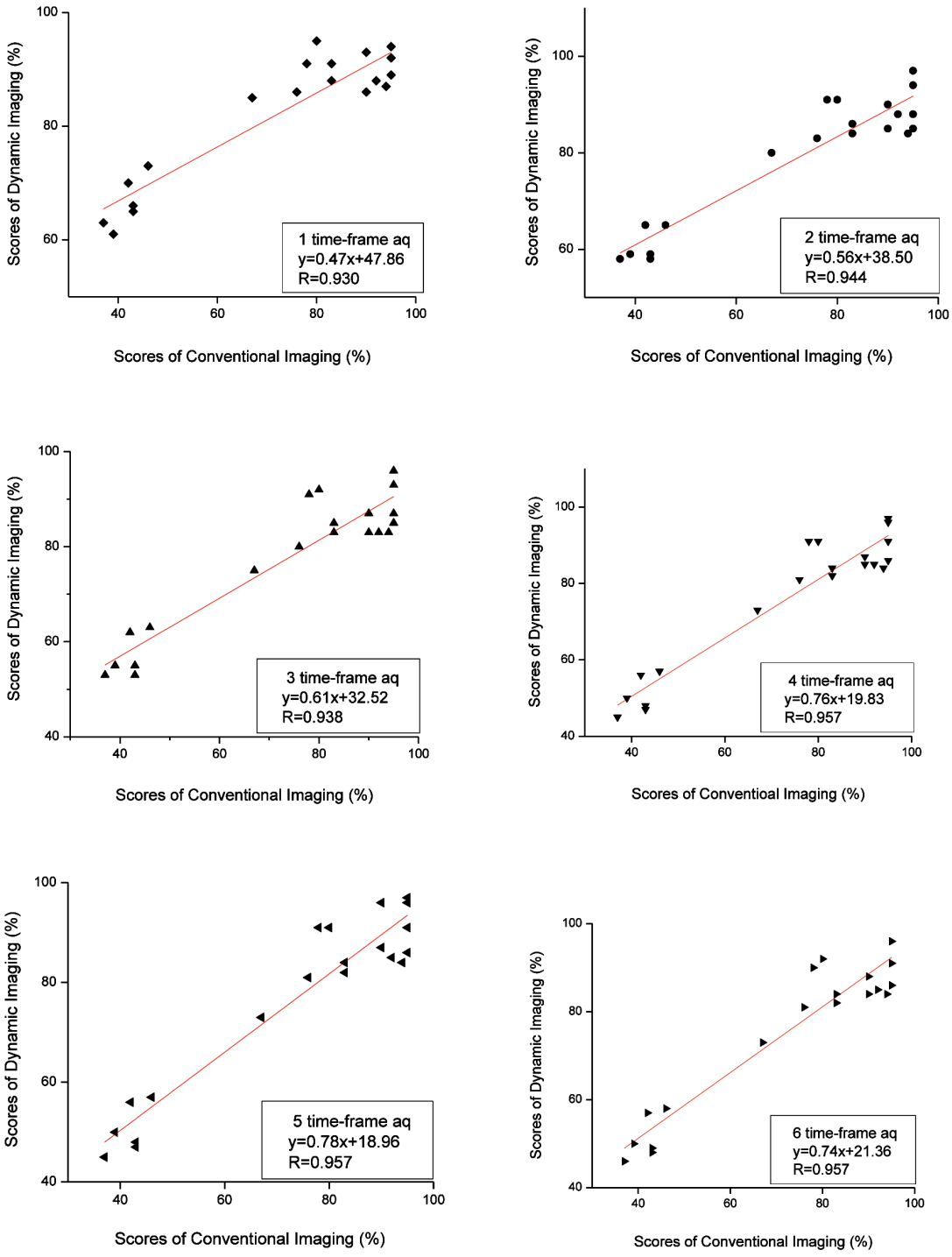

Figure 3. Correlation curves of comparison of Dynamic SPECT images using 1 to 6 time-frame acquisition protocol and conventional SPECT protocol in the context of perfusion test.

Correlation of results obtained using dynamic vs. conventional static protocols was actually poor for scans with little delay post-injection (figure 4). Correlations are clearly improved with increasing start times, reaching acceptable levels >200s post-injection.

3.2. Case Studies

The results of dynamic SPECT acquisition as performed on three cases are shown in Table 3. As previously described, three rotations were performed and MLEM reconstruction as applied to summation of the tomographic data was utilized (4 iterations).

Table 1. Absolute difference percentage in uptake values for different time frames of dynamic SPECT vs. conventional methods. Mean values of perfusion scores across 20 different myocardium segments are also shown.

Time Frames / Myocardial Segments	T†=1	T=2	T=3	T=4	T=5	T=6	Perfusion scores mean values (%)
B-anterior	-22	-11	-11	-11	-16	-20	-15.2
B-antroseptal	-26	-9	-8	-8	-16	-21	-14.2
B-inferoseptal	-27	-12	-11	-11	-17	-19	-16.2
B-inferior	-28	-15	-14	-14	-20	-23	-19
B-inferiolateral	-23	-6	-5	-5	-10	-16	-10.8
Basal	-22	-5	-4	-4	-12	-15	-10.3
M-anterior	-13	-12	-13	-13	-13	-13	-12.8
M-antroseptal	-18	-6	-6	-6	-8	-13	-9.5
M-inferoseptal	-10	-5	-5	-5	-4	-7	-6
M-inferior	-15	-12	-11	-11	-12	-11	-12
M-inferiolateral	-8	-1	-1	-1	-2	-3	-2.7
Mid	-5	1	1	1	0	-1	-0.5
D-anterior	3	-1	-2	-2	2	1	0.2
D-antroseptal	-3	2	3	3	3	0	1.3
D-inferoseptal	4	7	7	7	9	4	6.3
D- inferior	1	-1	-1	-1	-1	-2	-0.8
D- inferiolateral	7	10	10	10	11	10	9.7
Distal	6	9	9	9	10	10	8.8
A- anterior	6	4	4	4	8	7	5.5
A- inferior	4	6	-6	5	7	5	3.5

†: Time-frame(s)

B: Basal, M: Mid, D: Distal, A: Apical

Table 2. Absolute difference percentage in uptake values for different imaging start times post-injection between dynamic and static SPECT.

Myocardial Segments	t=0	t=32	t=64	t=96	t=128	t=160	t=192	t=224	t=256	t=288	t=320	t=384	t=352	t=416	t=448
B anterior	-7	-2	-12	-18	-22	-31	-24	-23	-16	-14	-2	4	0	4	5
B-antroseptal	-50	-55	-56	-56	-51	-35	-27	-24	-15	-13	0	6	1	4	6
B-inferoseptal	-15	-30	-36	-39	-35	-35	-28	-25	-15	-15	0	7	1	5	9
B-inferior	-17	-4	-11	-21	-27	-37	-29	-26	-17	-18	-4	5	-2	2	6
B-inferiolateral	-35	-37	-39	-42	-41	-35	-24	-20	-11	-10	1	9	4	8	11
Basal	12	12	4	-6	-13	-33	-24	-20	-11	-9	1	9	4	8	10
M-anterior	-12	5	3	-1	-8	-13	-12	-15	-13	-12	-3	4	0	3	6
M- antroseptal	-16	-25	-27	-26	-24	-24	-20	-19	-12	-9	1	7	3	7	11
M- inferosep-tal	-6	-5	-6	-8	-7	-13	-11	-11	-7	-5	1	7	3	6	9
M- inferior	27	25	14	3	-8	-16	-14	-16	-13	-11	-6	0	-4	-1	3
M- inferiolat-eral	13	4	3	0	-5	-10	-9	-8	-4	-4	3	7	5	8	10
Mid	34	34	20	8	0	-8	-5	-6	-2	-2	6	11	8	11	13
D- anterior	8	34	31	19	3	5	3	0	0	1	2	4	1	2	2
D- antroseptal	6	1	5	5	-5	-5	-4	-4	-1	1	5	8	6	9	10
D- inferoseptal	11	9	8	7	2	1	2	1	5	6	9	11	10	11	11
D- inferior	30	44	32	22	1	2	0	-3	-1	-2	-2	-1	-1	-2	-1
D- inferiolat-eral	45	24	19	14	0	4	5	4	8	8	9	9	9	10	9
Distal	42	28	21	15	2	4	5	3	8	7	10	11	10	11	10
A- anterior	12	35	26	15	3	4	6	3	5	5	6	9	6	6	7
A- inferior	6	28	22	11	-3	1	4	2	4	5	7	10	7	7	6

t: starting imaging time after injection

B: Basal, M: Mid, D: Distal, A: Apical

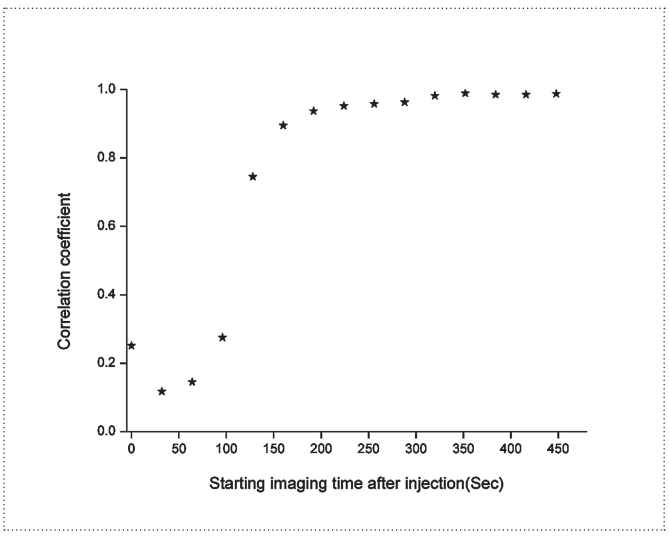

Figure 4. Correlation coefficient between dynamic and conventional perfusion SPECT imaging for different starting imaging times post-injection. Total scan time was fixed to be 192 s (3 camera rotations total).

First case was a 25 years old female. Second case was a 50 years old male with a preious MI (Myocardial Iscimia) in LAD (left anterior descending artery). Third case was a 69 years old male with a Severe MI in LAD and RCA (Right Coronary Artery).

After thallium scan of the cardium, in the first case, all segments were reported normal. In the second case, antroseptal and apex segments were found nonviable. While inferoseptal and inferior parts were reported viable. In the third case, all areas including apex, inferior, inferiolateral and septal basal were seen as nonviable

Table 3. Perfusion scores percent differences in uptake values for clinical dynamic vs. conventional SPECT.

Myocardial Segments	First case	Second case	Third case
B-anterior	-9	-6	0
B-antroseptal	-8	-5	-2
B-inferoseptal	-5	-2	-1
B-inferior	-2	-2	-5
B-inferiolateral	-13	-4	-1
Basal	-14	0	-2
M-anterior	-3	-5	-10
M-antroseptal	-2	3	-2
M-inferoseptal	-6	5	-2
M-inferior	-9	10	0
M-inferiolateral	-5	11	5
Mid	-2	-1	-9
D-anterior	-3	-8	-12
D-antroseptal	-2	-2	-3
D-inferoseptal	-8	-2	7
D-inferior	-4	-1	13
D-inferiolateral	-1	0	7
Distal	2	-9	-6
A-anterior	1	-12	-5
A-inferior	-5	-9	0
Imaging start time after injection (s)	**84**	**210**	**270**
Correlation	**0.571**	**0.948**	**0.960**

B: Basal, M: Mid, D: Distal, A: Apical

tissue. However, mid-septal segment was still viable. Overally, the patient had a severe overal infarction.

Based on the blind diagnosis of two nuclear medicine specialists, there was no significant difference between the two perfusion images either in defective or healthy regions. Moreover, in the terms of myocardial viability survey, there was no report on any considerable difference in any segment. Therefore, specialist's diagnosis confirmed the qualitative correspondence of dynamic and conventional imaging results.

Figure 5 demonstrates the bull's eye map of perfusion scores for a patient, comparing results from dynamic vs. conventional acquisition modes.

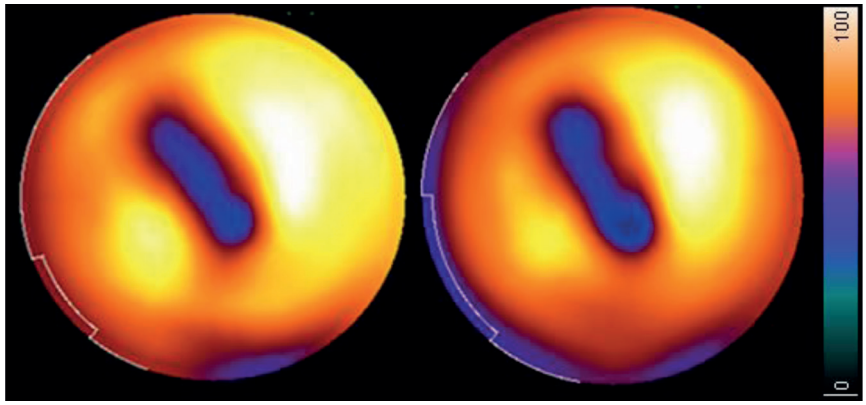

Figure 5. Bull's eye maps of the QPS analysis for a case study. Results are shown for the dynamic (Left) and conventional (Right) imaging protocols (case number 2).

4. Discussion

The study of physiological function of organ(s) of interest is one of the major goals of nuclear medicine imaging. In the conventional method, imaging begins after a time interval after the tracer injection. Over this period, the radiotracer has time to accumulate in the organ(s) of interest.

The study of cardiac perfusion, using dynamic imaging, however, offers additional functional information, as it may capture the kinetics of tracer transport and uptake, and can provide quantitative values more reflective of the underlying chemical and physiological mechanisms of interest. In conventional methods, the imaging protocols are typically based on one slow tomographic rotation performed following long delay times, and considerable kinetic information may be lost.

We wish to note that dynamic acquisition and imaging is expected to be more viable and powerful, and more likely to be adopted for routine and widespread usage, if it can be demonstrated to maintain capabilities of traditional static perfusion imaging.

We thus set to investigate the feasibility of perfusion imaging via dynamic SPECT in simulations and clinical studies using a dual-head SPECT system. In order to do this, we performed a summation of dynamically obtained tomographic data. The results of comparisons between dynamic and conventional imaging indicated a very good correlation between the two imaging methods, especially when using more than three time-frames and with data acquired >5 minutes post-injection. Furthermore, a comparison of perfusion scores between the two methods indicated that dynamic MPI values in most basal and mid regions were amplified. Because an increase in frame numbers beyond 4 (64 sec for each cycle) did not improve the correlation coefficient, a reasonably shortened total duration was necessary to achieve myocardial perfusion assessment comparable to conventional imaging.

If appropriate acquisition delay post-injection is not observed (~150 sec or more), correlations were poor, which is clearly related to the fact that at early times the blood activity exceeds that of myocardial tissue activity, and there are different underlying spill-in/out processes at play, and there may not be enough uptake in the myocardium for constant total duration protocols. However, Tang et al.[49] did demonstrate (in Rb-82 PET imaging) that using less delay (but not ending earlier; i.e. maintaining typical end of acquisition times) actually enhanced perfusion defect detection, even though it resulted in images with less or even no contrast between the myocardium and blood pool.

As it is shown in table 3, dynamic imaging showed higher perfusion score in most of the segments compared to the conventioanl imaging. The average of perfusion score differences was 2.75±5.54%. The relatively lower correlation between dynamic and conventional results for the case of the healthy volunteer may have been due to the short dely post-injection. According to our results, the optimum time to start acquisition was beyond 200s post-injection, while for this case it was only 84 sec. In the interval of about 3 min post-injection, the blood activity curve typically reaches its maximun, and there may not have been enough time to absorb a significant amount of thallium in the myocardium.

As mentioned before, the myocardial thallium scan is a conventional method for viability assessment. The perfusion images of dynamic method were compared with the conventional results, both quantitavely and qualitatively. There were no significant difference between the dynamic and conventioal results. Moreover, dynamic images have the capability to extract the timing information of the region of interest.

Finally, we must note that the next clear line of research is to pursue the capabilities that dynamic SPECT imaging provides beyond conventional imaging. Clearly, this area requires careful optimization for specific tasks of interest (e.g. detection, quantification) and one may discover that different start-time delays and total durations may be required for optimal kinetic parameter estimation. Subsequent to this, the results of the present work must be put in perspective with new results, and the relative importance of the different kinds of images and parameters estimated need to be assessed in orderto propose viable and appropriate acquisition protocols.

5. Conclusion

Dynamic image acquisition opens up new opportunities for estimation of kinetic parameters and processes of interest. Dynamic SPECT, as the recent works demonstrate, has valuable kinetic information about the organ of interest. However, for the acquired data from cardiac dynamic SPECT technique, myocardial perfusion also affects tracer kinetics to some extent. Form this phenomenon a hypothesis arises whether it is possible to generate conventional perfusion scores and kinetic information simultaneously with cardiac dynamic SPECT technique. This is a notable consideration because it enables more widespread adoption of this technique, as it maintains the capability to generate conventional perfusion scores, while it enables additional generation of kinetic parameters of interest.

At the present work, we seek the correlation of perfusion scores extracted from dynamic SPECT techniques with conventional methods, using Monte Carlo simulation and case studies. As the results show, the dynamic SPECT methods can be utilized to produce perfusion images that are highly correlated with conventional SPECT imaging. The reliable myocardial perfusion information with additional kinetic parameters at the same time may treat more widespread utilization of dynamic SPECT techniques.

Acknowledgment

This work was supported in part by the Cardiovascular Interventional Research Center, Department of Nuclear Medicine, Medical & Research Center, Rajaei Cardiovascular Hospital. The authors would like to thank Dr. Seyed Hassan Firuzabadi for providing usage of equipment and for his advice and consultation. The authors also would like to thank Mr. Mahani for his helpful comments and the personnel at Rajaei's Hospital, Tehran, Iran, particularly Mr. Ali-Poor and Mr. Moosa-Zade for their assistance in acquiring the case data.

References

[1] A. Rahmim and H. Zaidi, "PET versus SPECT: strengths, limitations and challenges," Nucl. Med. Comm., vol. 29, pp. 193-207, 2008.

[2] A. Celler, T. Farncombe, C. Bever, D. Noll, J. Maeght, R. Harrop, et al., "Performance of the dynamic single photon emission computed tomography (dSPECT) method for decreasing or increasing activity changes," Phys Med Biol, vol. 45, pp. 3525-43, 2000.

[3] S. G. Ross, A. Welch, G. T. Gullberg, and R. H. Huesman, "An investigation into the effect of input function shape and image acquisition interval on estimates of washin for dynamic cardiac SPECT," Phys Med Biol, vol. 42, pp. 2193-213, Nov 1997.

[4] G. T. Gullberg, B. W. Reutter, A. Sitek, J. S. Maltz, and T. F. Budinger, "Dynamic single photon emission computed tomography—basic principles and cardiac applications," Phys. Med. Biol., vol. 55, pp. 111-119, 2010.

[5] M. P. Hudon, D. M. Lyster, E. W. Jamieson, K. A. Qayumi, M. C. Kiess, L. J. Rosado, et al., "Efficacy of 15-(123I)-p-iodophenyl pentadecanoic acid (IPPA) in assessing myocardial metabolism in a model of reversible global ischemia," Eur J Nucl Med, vol. 14, pp. 594-9, 1988.

[6] S. H. Nellis, A. J. Liedtke, and B. Renstrom, "Fatty acid kinetics in aerobic myocardium: characteristics of tracer carbon entry and washout and influence of metabolic demand," J Nucl Med, vol. 33, pp. 1864-74, 1992.

[7] Y. Zan, B. R., Q. Huang, B. Li, K. Chen, and G. T. Gullberg, "Fast direct estimation of the blood input function and myocardial time activity curve from dynamic SPECT projections via reduction in spatial and temporal dimensions," Med Phys, vol. 40, p. 092503, 2013.

[8] D. J. Gerven, A. N. Schneider, D. M. Wuitchik, and R. W. Skelton, "Direct measurement of spontaneous strategy selection in a virtual Morris water maze shows females choose an allocentric strategy at least as often as males do," Behav Neurosci, vol. 126, pp. 465-78, Jun 2012.

[9] D. S. Berman, L. J. Shaw, J. K. Min, R. Hachamovitch, A. Abidov, G. Germano, et al., "SPECT/PET myocardial perfusion imaging versus coronary CT angiography in patients with known or suspected CAD," Q J Nucl Med Mol Imaging, vol. 54, pp. 177-200, 2010.

[10] A. Elhendy, J. J. Bax, and D. Poldermans, "Dobutamine stress myocardial perfusion imaging in coronary artery disease," J Nucl Med, vol. 43, pp. 1634-46, 2002.

[11] E. G. DePuey, E. V. G., and D. S. B., Cardiac SPECT Imaging, Second ed.: Lippincott Williams & Wilkins, 2001.

[12] K. Nakajima, J. Taki, H. Bunko, M. Matsudaira, A. Muramori, I. Matsunari, et al., "Dynamic acquisition with a three-headed SPECT system: application to technetium 99m-SQ30217 myocardial imaging," J Nucl Med, vol. 32, pp. 1273-7, 1991.

[13] N. Tomoaki, H. Akiyoshi, W. Takeru, K. Hideo, and N. Tsunehiko, "Prediction of New-Onset Refractory Congestive Heart Failure Using Gated Myocardial Perfusion SPECT Imaging in Patients With Known or Suspected Coronary Artery DiseaseSubanalysis of the J-ACCESS Database," JACC: Cardiovascular Imaging, vol. 2, pp. 1393-1400, 2009.

[14] L. Z. Barry and G. A. Beller, Clinical Nuclear Cardiology: State of the Art and Future Directions, fourth ed. Philadelphia: ELSEVIER, 2010.

[15] J. Chen, J. R. Galt, J. N. Aarsvold, E. G. Krawczynska, N. P. Alazraki, A. M. Zafari, et al., "Dynamic Cardiac SPECT With Tc-99m Teboroxime: Compensation for Rapid Myocardial Washout and High Liver Uptake," IEEE Transections on Nuclear Science, vol. 51, pp. 2705-2713, October 2004 2004.

[16] A. Beller, Clinical Nuclear Cardiology: State of the Art and Future Directions, fourth ed.: ELSEVIER, 2010.

[17] G. Friedlander, J. W. Kennedy, E. S. Macias, and J. M. Miller, Nuclear and Radiochemistry: Wiley, 1981.

[18] G. V. Heller, A. Mann, and R. C. Hendel, Nuclear cardiology, 2000.

[19] R. J. Kowalski, Radio-pharmaceuticals in nuclear medicine practice. California: Appleton & Lange, 1987.

[20] R. K. Narra, A. D. Nunn, B. L. Kuczynski, T. Feld, P. Wedeking, and W. C. Eckelman, "A neutral technetium-99m complex for myocardial imaging," J Nucl Med, vol. 30, pp. 1830-7, 1989.

[21] D. J. Kadrmas, E. V. R. Di Bella, H. S. Khare, P. E. Christian, and G. T. Gullberg, "Static versus dynamic teboroxime myocardial perfusion SPECT in canines," in Nuclear Science Symposium, 1999. Conference Record. 1999 IEEE, 1999, pp. 1292-1296.

[22] W. C. Eckelman, J. Steigman, and C. Paik, Radiopharmaceutical Chemistry, In Nuclear Medicine, Diagnosis and Therapy. New York: Thieme Medical Publishers, Inc., 1996.

[23] G. A. Beller and S. R. Bergmann, "Myocardial perfusion imaging agents: SPECT and PET," J Nucl Cardiol, vol. 11, pp. 71-86, 2004.

[24] D. J. Kadrmas, E. V. R. DiBella, H. S. Khare, P. E. Christian, and G. T. Cullberg, "Static versus dynamic teboroxime myocardial perfusion SPECT in canines," Nuclear Science, IEEE Transactions on, vol. 47, pp. 1112-1117, 2000.

[25] H. S. Khare, E. V. Dibella, D. J. Kadrmas, P. E. Christian, and G. T. Gullberg, "Comparison of Static and Dynamic Cardiac Perfusion Thallium-201 SPECT," IEEE Trans Nucl Sci, vol. 48, pp. 774-790, Jun 2001.

[26] X. Niu, Y. Yang, and M. Jin, "Fully 5d reconstruction of gated dynamic cardiac SPECT images using temporal B-splines," in Biomedical Imaging: From Nano to Macro, 2010 IEEE International Symposium on, 2010, pp. 460-463.

[27] X. Niu, Y. Yang, and M. A. King, "Comparison study of temporal regularization methods for fully 5D reconstruction of cardiac gated dynamic SPECT," Phys Med Biol, vol. 57, pp. 5523-5542, Aug 8 2012.

[28] X. Niu, Y. Yang, M. A. King, and M. N. Wernick, "Detectability of perfusion defect in five-dimensional gated-dynamic cardiac SPECT images," Med Phys, vol. 37, pp. 5102-12, Sep 2010.

[29] M. Jin, Y. Yang, and M. A. King, "Reconstruction of dynamic gated cardiac SPECT," Med Phys, vol. 33, pp. 4384-94, Nov 2006.

[30] P. C. Chiao, E. P. Ficaro, F. Dayanikli, W. L. Rogers, and M. Schwaiger, "Compartmental analysis of technetium-99m-teboroxime kinetics employing fast dynamic SPECT at rest and stress," J Nucl Med, vol. 35, pp. 1265-73, 1994.

[31] B. W. Reuttery, G. T. Gullbergz, and R. H. Huesmany, "Kinetic Parameter Estimation from Dynamic Cardiac Patient SPECT Projection Measurements," presented at the IEEE Nuclear Science Symposium and Medical Imaging Conference, Toronto, Ont., 1998.

[32] A. M. Smith, G. T. Gullberg, P. E. Christian, and L. Datz, "Kinetic modeling of teboroxime using dynamic SPECT imaging of a canine model," J. Nucl. Med, vol. 35, pp. 484-95, 1994.

[33] G. L. Zeng, A. Hernandez, D. J. Kadrmas, and G. T. Gullberg, "Kinetic parameter estimation using a closed-form expression via integration by parts," Phys Med Biol, vol. 57, pp. 5809-21, 2012.

[34] R. Klein, "Kinetic Model Based Factor Analysis of Cardiac 82Rb PET Images for Improved Accuracy of Quantitative Myocardial Blood Flow Measurement.," PhD, School of Information Technology and Engineering, University of Ottawa, 2010.

[35] F. Alhassen, N. Nguyen, S. Bains, R. G. Gould, Y. Seo, S. L. Bacharach, et al., "Myocardial blood flow measurement with a conventional dual-head SPECT/CT with spatiotemporal iterative reconstructions - a clinical feasibility study," Am J Nucl Med Mol Imaging, vol. 4, pp. 53-9, 2013.

[36] T. Humphries, "Temporal regularization and artifact correction in single slowrotation dynamic SPECT," Doctor of Philosophy, Simon Fraser University, 2011.

[37] D. Y. Riabkov and E. V. R. Di Bella, "Estimation of kinetic parameters without input functions: analysis of three methods for multichannel blind identification," Biomedical Engineering, IEEE Transactions on, vol. 49, pp. 1318-1327, 2002.

[38] R. C. Marshall, P. Powers-Risius, B. W. Reutter, S. E. Taylor, H. F. Van-Brocklin, R. H. Huesman, et al., "Kinetic analysis of 125I-iodorotenone as a deposited myocardial flow tracer: comparison with 99mTc-sestamibi," J. Nucl. Med., vol. 42, pp. 272-281, 2001.

[39] G. T. Gulberg, R. H. Huesman, and G. L. Zeng, "Efficient estimation of dynamic cardiac SPECT kinetic parameters using singular value decomposition reconstruction," presented at the Annual meeting of the Society of Nuclear Medicine, Orlando, FL (United States), 1994.

[40] W. P. Segars, "Development and Application of the New Dynamic NURBS-based Cardiac-Torso (NCAT) Phantom " Ph. D. Dissertation, Johns Hopkins Outpatient Center The University of North Carolina at Chapel Hill 2001.

[41] H. Iida, S. Eberl, K. M. Kim, Y. Tamura, Y. Ono, M. Nakazawa, et al., "Absolute quantitation of myocardial blood flow with (201)Tl and dynamic SPECT in canine: optimisation and validation of kinetic modelling," Eur J Nucl Med Mol Imaging, vol. 35, pp. 896-905, 2008.

[42] M. Mamede, E. Tadamura, R. Hosokawa, M. Ohba, S. Kubo, M. Yamamuro, et al., "Comparison of myocardial blood flow induced by adenosine triphosphate and dipyridamole in patients with coronary artery disease," Ann Nucl Med, vol. 19, pp. 711-7, 2005.

[43] M. Ljungberg, Monte Carlo Calculations in Nuclear Medicine, Second Edition: Applications in Diagnostic Imaging. Florence: Taylor & Francis, 2012.

[44] K. Sundin and M. Ljungberg, "SIMIND based pinhole imaging: Development and validation," in Nuclear Science Symposium Conference, 2007, pp. 3998-4005.

[45] C. A. Giannone, "Monte Carlo Calculations in Nuclear Medicine: Applications in Diagnostic Imaging," Physiological Measurement, vol. 20, 1999.

[46] Z. Cao, C. Maunoury, C. C. Chen, and L. E. Holder, "Comparison of continuous step-and-shoot versus step-and-shoot acquisition SPECT," J Nucl Med, vol. 37, pp. 2037-40, 1996.

[47] S. G. Ross, A. Welch, G. T. Gullberg, and R. H. Huesman, "An investigation into the effect of input function shape and image acquisition interval on estimates of washin for dynamic cardiac SPECT," Phys Med Biol, vol. 42, p. 2193, 1997.

[48] F. Kalantari, H. Rajabi, and N. Yaghoobi, "Optimized Energy Window Configuration for 201Tl Imaging," J. Nucl. Med. Technol., vol. 36, pp. 36-44, March 2008 2008.

[49] J. Tang, A. Rahmim, R. Lautamäki, M. A. Lodge, F. M. Bengel, and B. M. W. Tsui, "Optimization of Rb-82 PET acquisition and reconstruction protocols for myocardial perfusion defect detection," Phys. Med. Biol., vol. 54, pp. 3161-71, 2009.